

Measurement of EPR-type flavour entanglement in $\Upsilon(4S) \rightarrow B^0 \bar{B}^0$ decays

A. Go,²² A. Bay,¹⁶ K. Abe,⁷ H. Aihara,⁴³ D. Anipko,¹ V. Aulchenko,¹ T. Aushev,^{16,12}
 A. M. Bakich,³⁸ E. Barberio,¹⁹ K. Belous,¹¹ U. Bitenc,¹³ I. Bizjak,¹³ S. Blyth,²² A. Bozek,²⁵
 M. Bračko,^{7,18,13} T. E. Browder,⁶ P. Chang,²⁴ Y. Chao,²⁴ A. Chen,²² K.-F. Chen,²⁴
 W. T. Chen,²² B. G. Cheon,² R. Chistov,¹² Y. Choi,³⁷ Y. K. Choi,³⁷ S. Cole,³⁸ J. Dalseno,¹⁹
 M. Danilov,¹² M. Dash,⁴⁷ A. Drutskoy,³ S. Eidelman,¹ D. Epifanov,¹ S. Fratina,¹³ N. Gabyshev,¹
 T. Gershon,⁷ G. Gokhroo,³⁹ B. Golob,^{17,13} A. Gorišek,¹³ H. Ha,¹⁴ N. C. Hastings,⁴³
 K. Hayasaka,²⁰ H. Hayashii,²¹ M. Hazumi,⁷ D. Heffernan,³⁰ T. Hokuue,²⁰ Y. Hoshi,⁴¹ S. Hou,²²
 W.-S. Hou,²⁴ T. Iijima,²⁰ K. Ikado,²⁰ A. Imoto,²¹ K. Inami,²⁰ A. Ishikawa,⁴³ H. Ishino,⁴⁴
 R. Itoh,⁷ M. Iwasaki,⁴³ Y. Iwasaki,⁷ C. Jacoby,¹⁶ J. H. Kang,⁴⁸ N. Katayama,⁷ T. Kawasaki,²⁷
 H. R. Khan,⁴⁴ H. Kichimi,⁷ H. J. Kim,¹⁵ S. K. Kim,³⁵ Y. J. Kim,⁵ K. Kinoshita,³ S. Korpar,^{18,13}
 P. Križan,^{17,13} P. Krokovny,⁷ R. Kulasiri,³ R. Kumar,³¹ C. C. Kuo,²² A. Kuzmin,¹ Y.-J. Kwon,⁴⁸
 J. S. Lange,⁴ J. Lee,³⁵ M. J. Lee,³⁵ T. Lesiak,²⁵ A. Limosani,⁷ S.-W. Lin,²⁴ Y. Liu,⁵
 D. Liventsev,¹² T. Matsumoto,⁴⁵ A. Matyja,²⁵ S. McOnie,³⁸ W. Mitaroff,¹⁰ H. Miyake,³⁰
 H. Miyata,²⁷ Y. Miyazaki,²⁰ R. Mizuk,¹² T. Mori,²⁰ E. Nakano,²⁹ M. Nakao,⁷ Z. Natkaniec,²⁵
 S. Nishida,⁷ O. Nitoh,⁴⁶ S. Ogawa,⁴⁰ T. Ohshima,²⁰ S. L. Olsen,⁶ Y. Onuki,³³ P. Pakhlov,¹²
 G. Pakhlova,¹² H. Palka,²⁵ C. W. Park,³⁷ H. Park,¹⁵ L. S. Peak,³⁸ R. Pestotnik,¹³ M. Peters,⁶
 L. E. Piilonen,⁴⁷ H. Sahoo,⁶ Y. Sakai,⁷ N. Satoyama,³⁶ T. Schietinger,¹⁶ O. Schneider,¹⁶
 J. Schümann,²³ A. J. Schwartz,³ R. Seidl,^{8,33} K. Senyo,²⁰ M. Shapkin,¹¹ H. Shibuya,⁴⁰
 B. Shwartz,¹ J. B. Singh,³¹ A. Somov,³ N. Soni,³¹ S. Stanič,²⁸ M. Starič,¹³ H. Stoeck,³⁸
 T. Sumiyoshi,⁴⁵ F. Takasaki,⁷ M. Tanaka,⁷ G. N. Taylor,¹⁹ Y. Teramoto,²⁹ X. C. Tian,³²
 I. Tikhomirov,¹² K. Trabelsi,⁶ T. Tsuboyama,⁷ T. Tsukamoto,⁷ S. Uehara,⁷ T. Uglov,¹²
 K. Ueno,²⁴ Y. Unno,² S. Uno,⁷ G. Varner,⁶ S. Villa,¹⁶ C. C. Wang,²⁴ C. H. Wang,²³
 M.-Z. Wang,²⁴ Y. Watanabe,⁴⁴ J. Wicht,¹⁶ E. Won,¹⁴ Q. L. Xie,⁹ B. D. Yabsley,³⁸
 A. Yamaguchi,⁴² Y. Yamashita,²⁶ M. Yamauchi,⁷ Z. P. Zhang,³⁴ V. Zhilich,¹ and A. Zupanc¹³

(The Belle Collaboration)

¹*Budker Institute of Nuclear Physics, Novosibirsk*²*Chonnam National University, Kwangju*³*University of Cincinnati, Cincinnati, Ohio 45221*⁴*Justus-Liebig-Universität Gießen, Gießen*⁵*The Graduate University for Advanced Studies, Hayama*⁶*University of Hawaii, Honolulu, Hawaii 96822*⁷*High Energy Accelerator Research Organization (KEK), Tsukuba*⁸*University of Illinois at Urbana-Champaign, Urbana, Illinois 61801*⁹*Institute of High Energy Physics, Chinese Academy of Sciences, Beijing*¹⁰*Institute of High Energy Physics, Vienna*¹¹*Institute of High Energy Physics, Protvino*¹²*Institute for Theoretical and Experimental Physics, Moscow*¹³*J. Stefan Institute, Ljubljana*¹⁴*Korea University, Seoul*¹⁵*Kyungpook National University, Taegu*¹⁶*Swiss Federal Institute of Technology of Lausanne, EPFL, Lausanne*¹⁷*University of Ljubljana, Ljubljana*

¹⁸*University of Maribor, Maribor*
¹⁹*University of Melbourne, Victoria*
²⁰*Nagoya University, Nagoya*
²¹*Nara Women's University, Nara*
²²*National Central University, Chung-li*
²³*National United University, Miao Li*
²⁴*Department of Physics, National Taiwan University, Taipei*
²⁵*H. Niewodniczanski Institute of Nuclear Physics, Krakow*
²⁶*Nippon Dental University, Niigata*
²⁷*Niigata University, Niigata*
²⁸*University of Nova Gorica, Nova Gorica*
²⁹*Osaka City University, Osaka*
³⁰*Osaka University, Osaka*
³¹*Panjab University, Chandigarh*
³²*Peking University, Beijing*
³³*RIKEN BNL Research Center, Upton, New York 11973*
³⁴*University of Science and Technology of China, Hefei*
³⁵*Seoul National University, Seoul*
³⁶*Shinshu University, Nagano*
³⁷*Sungkyunkwan University, Suwon*
³⁸*University of Sydney, Sydney NSW*
³⁹*Tata Institute of Fundamental Research, Mumbai*
⁴⁰*Toho University, Funabashi*
⁴¹*Tohoku Gakuin University, Tagajo*
⁴²*Tohoku University, Sendai*
⁴³*Department of Physics, University of Tokyo, Tokyo*
⁴⁴*Tokyo Institute of Technology, Tokyo*
⁴⁵*Tokyo Metropolitan University, Tokyo*
⁴⁶*Tokyo University of Agriculture and Technology, Tokyo*
⁴⁷*Virginia Polytechnic Institute and State University, Blacksburg, Virginia 24061*
⁴⁸*Yonsei University, Seoul*

(Dated: December 18, 2018)

Abstract

The neutral B -meson pair produced at the $\Upsilon(4S)$ should exhibit a non-local correlation of the type discussed by Einstein, Podolski, and Rosen. We measure this correlation using the time-dependent flavour asymmetry of semileptonic B^0 decays, which we compare with predictions from quantum mechanics and two local realistic models. The data are consistent with quantum mechanics, and inconsistent with the other models. Assuming that some B pairs disentangle to produce B^0 and \overline{B}^0 with definite flavour, we find a decoherent fraction of 0.029 ± 0.057 , consistent with no decoherence.

PACS numbers: 03.65.Ud, 03.65.Yz, 13.25.Hw

The concept of entangled states, which cannot be described as product states of their parts, was born with Quantum Mechanics (QM). In 1935 Einstein, Podolski and Rosen (EPR) considered such a pair of particles and concluded that QM cannot be a “complete” theory [1]; this suggests that additional (“hidden”) variables are required. In 1964 J. S. Bell showed that QM can violate a certain inequality, which is (by contrast) satisfied by all local hidden variable models [2]. Many experiments have since been performed confirming such violation [3], including studies of the K -meson system [4]. In this paper, we present a study of EPR correlation in the flavour of B -meson pairs produced at the $\Upsilon(4S)$. A Bell inequality test cannot be performed [5] due to the rapid decrease in time of the B -meson amplitudes, and the passive character of the flavour measurement, *via* reconstruction of B -meson decay products. Instead, we compare the data with predictions from QM and other models.

The wavefunction of a $B^0\bar{B}^0$ pair from $\Upsilon(4S)$ decay is analogous to that of photons in a spin-singlet state [6, 7]:

$$|\psi\rangle = \frac{1}{\sqrt{2}} [|B^0\rangle_1 \otimes |\bar{B}^0\rangle_2 - |\bar{B}^0\rangle_1 \otimes |B^0\rangle_2]. \quad (1)$$

Decays occurring at the same proper time are fully correlated: the flavour-specific decay of one meson fixes the (previously undetermined) flavour B^0/\bar{B}^0 of the other meson. Given (1), the time-dependent rate for decay into two flavour-specific states $R_i = e^{-\Delta t/\tau_{B^0}}/(4\tau_{B^0})\{1 \pm \cos(\Delta m_d \Delta t)\}$ for opposite flavour ($B^0\bar{B}^0$; $+$, $i = \text{OF}$) and same flavour (B^0B^0 or $\bar{B}^0\bar{B}^0$; $-$, $i = \text{SF}$) decays. $\Delta t \equiv |t_1 - t_2|$ is the proper-time difference of the decays, and Δm_d the mass difference between the two B^0 - \bar{B}^0 mass eigenstates. We have assumed a lifetime difference $\Delta\Gamma_d = 0$ and neglected the effects of CP violation in mixing, which are $O(10^{-4})$ or less.

The time-dependent asymmetry is thus $A_{\text{QM}}(\Delta t) \equiv (R_{\text{OF}} - R_{\text{SF}}) / (R_{\text{OF}} + R_{\text{SF}}) = \cos(\Delta m_d \Delta t)$, a function of Δt but not the individual times $t_{1,2}$: a manifestation of entanglement. We compare the time-dependent asymmetry in data to this result and the predictions of

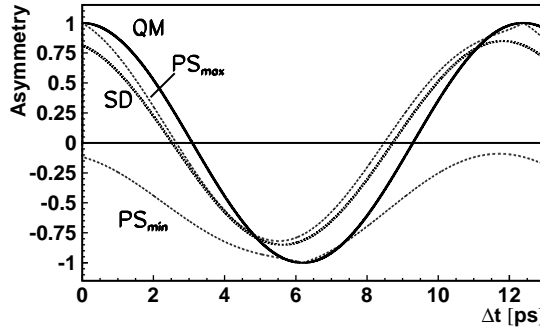


FIG. 1: Time-dependent asymmetry predicted by (QM) quantum mechanics and (SD) spontaneous and immediate disentanglement of the B -pair [8, 9], and (PS_{min} to PS_{max}) the range of asymmetries allowed by the Pompili-Selleri model [10]. $\Delta m_d = 0.507 \text{ ps}^{-1}$ is assumed [11].

two other models (Fig. 1).

In the Spontaneous and immediate Disentanglement model (SD), the B -meson pair separates into a B^0 and \bar{B}^0 with well-defined flavour immediately after the $\Upsilon(4S)$ decay, which then evolve independently [8]. We thus have complete “decoherence” [9] and the asymmetry becomes

$$\begin{aligned} A_{\text{SD}}(t_1, t_2) &= \cos(\Delta m_d t_1) \cos(\Delta m_d t_2) \\ &= \frac{1}{2} [\cos(\Delta m_d(t_1 + t_2)) + \cos(\Delta m_d \Delta t)], \end{aligned} \quad (2)$$

depending on $t_1 + t_2$ in addition to Δt . Due to the large uncertainty on the $\Upsilon(4S)$ decay point, it is difficult to measure individual decay times $t_{1,2}$: only Δt is measured in this analysis. Integrating over $t_1 + t_2$ gives the curve shown in Fig. 1.

In the local realistic model by Pompili and Selleri (PS) [10], each B has “elements of reality” with well-defined flavour, B^0 or \bar{B}^0 , and mass, corresponding to the heavy and light B^0 - \bar{B}^0 eigenstates. There are thus four basic states: B_H^0 , B_L^0 , \bar{B}_H^0 , \bar{B}_L^0 . The model imposes mass and flavour anti-correlations at equal times $\Delta t = 0$; mass values are stable, but there are random simultaneous jumps in flavour within the pair. Requiring that QM predictions for uncorrelated B -decays are reproduced, the asymmetry must then lie within the bounds

$$A_{\text{PS}}^{\text{max}}(t_1, t_2) = 1 - |\{1 - \cos(\Delta m_d \Delta t)\} \cos(\Delta m_d t_{\min}) + \sin(\Delta m_d \Delta t) \sin(\Delta m_d t_{\min})|, \text{ and} \quad (3)$$

$$A_{\text{PS}}^{\text{min}}(t_1, t_2) = 1 - \min(2 + \Psi, 2 - \Psi), \text{ where} \quad (4)$$

$$\Psi = \{1 + \cos(\Delta m_d \Delta t)\} \cos(\Delta m_d t_{\min}) - \sin(\Delta m_d \Delta t) \sin(\Delta m_d t_{\min}). \quad (5)$$

Note the additional $t_{\min} = \min(t_1, t_2)$ dependence. After integrating over t_{\min} we obtain the curves PS_{max} and PS_{min} shown in Fig. 1.

To determine the asymmetry, we use 152×10^6 $B\bar{B}$ pairs collected by the Belle detector at the $\Upsilon(4S)$ resonance at the KEKB asymmetric-energy (3.5 GeV on 8.0 GeV) e^+e^- collider [12]. The Belle detector [13] is a large-solid-angle spectrometer consisting of a silicon vertex detector (SVD), central drift chamber (CDC), aerogel Cherenkov counters (ACC), time-of-flight counters (TOF), and a CsI(Tl) electromagnetic calorimeter (ECL) inside a 1.5T superconducting solenoid. The flux return is instrumented to detect K_L^0 and identify muons (KLM). The $\Upsilon(4S)$ is produced with $\beta\gamma = 0.425$ close to the z axis (defined as anti-parallel to the positron beam line). As the B momentum is low in the $\Upsilon(4S)$ center-of-mass system (CMS), Δt can be determined from the z -displacement of B -decay vertices: $\Delta t \approx \Delta z / \beta\gamma c$.

We use an event selection similar to that of a previous Belle analysis [14, 15], but optimised for theoretical model discrimination; in particular we use tighter cuts on the flavour tag purity. To enable direct comparison of the result with different models, we subtract both background and mistagged-flavour events from the data, and then correct for detector effects by deconvolution.

We determine the flavour of one neutral B by reconstructing the decay $B^0 \rightarrow D^{*-} \ell^+ \nu$, with $D^{*-} \rightarrow \bar{D}^0 \pi_s^-$ and $\bar{D}^0 \rightarrow K^+ \pi^-(\pi^0)$ or $K^+ \pi^- \pi^+ \pi^-$ (charge-conjugate modes are included throughout this Letter). Charged particles (except the “slow pion” π_s) are chosen from tracks with associated SVD hits and radial impact parameter $dr < 0.2$ cm, and required to satisfy kaon/pion identification criteria using combined TOF, ACC and CDC (dE/dx) information. $\pi^0 \rightarrow \gamma\gamma$ candidates are selected with $|M_{\gamma\gamma} - m_{\pi^0}| < 11 \text{ MeV}/c^2$ and momenta $p_{\pi^0} > 0.2 \text{ GeV}/c$; the photons must have energies $E_\gamma > 80 \text{ MeV}$. We select D^0 candidates with $(M_{K\pi\pi} - m_{D^0}) \in [-13, 13] \text{ MeV}/c^2$ for $K\pi(\pi\pi)$ and $[-37, 23] \text{ MeV}/c^2$ for $K\pi\pi^0$. A D^* candidate is formed by constraining a D^0 and slow pion to a common vertex. We require a mass difference $M_{\text{diff}} = M_{K\pi\pi_s} - M_{K\pi\pi} \in [144.4, 146.4] \text{ MeV}/c^2$, and CMS momentum $p_{D^*}^* < 2.6 \text{ GeV}/c$, consistent with B -decay. Electron identification uses momentum and dE/dx information, ACC response, and energy deposition in the ECL. Muon identification is based on penetration depth and matching of hits in the KLM to the extrapolated track. The efficiency is about 92% (84%) for electrons (muons) in the relevant momentum region, from 1.4 to 2.4 GeV/c in the CMS; hadrons pass this selection with an efficiency of 0.2% (1.1%). We require that the CMS angle between the D^* and lepton be greater than 90° . From the relation $M_\nu^2 = (E_\nu^* - E_{D^*\ell}^*)^2 - |\vec{p}_B^*|^2 - |\vec{p}_{D^*\ell}^*|^2 + 2|\vec{p}_B^*||\vec{p}_{D^*\ell}^*| \cos(\theta_{B,D^*\ell})$, where $\theta_{B,D^*\ell}$ is the angle between \vec{p}_B^* and $\vec{p}_{D^*\ell}^*$, we can reconstruct $\cos(\theta_{B,D^*\ell})$ by assuming a vanishing neutrino mass. We require $|\cos(\theta_{B,D^*\ell})| < 1.1$. The neutral B decay position is determined by fitting the lepton track and

TABLE I: Time-dependent asymmetry in Δt bins, corrected for experimental effects, with statistical and systematic uncertainties. Contributions from event selection, background subtraction, wrong tag correction, and deconvolution are also shown.

Δt bin	window [ps]	A and total error	stat. error	Systematic errors				
				total	event sel.	bkgd sub.	wrong tags	deconvol.
1	0.0 – 0.5	1.013 ± 0.028	0.020	0.019	0.005	0.006	0.010	0.014
2	0.5 – 1.0	0.916 ± 0.022	0.015	0.016	0.006	0.007	0.010	0.009
3	1.0 – 2.0	0.699 ± 0.038	0.029	0.024	0.013	0.005	0.009	0.017
4	2.0 – 3.0	0.339 ± 0.056	0.047	0.031	0.008	0.005	0.007	0.029
5	3.0 – 4.0	-0.136 ± 0.075	0.060	0.045	0.009	0.009	0.007	0.042
6	4.0 – 5.0	-0.634 ± 0.084	0.062	0.057	0.021	0.014	0.013	0.049
7	5.0 – 6.0	-0.961 ± 0.077	0.060	0.048	0.020	0.017	0.012	0.038
8	6.0 – 7.0	-0.974 ± 0.080	0.060	0.053	0.034	0.025	0.020	0.025
9	7.0 – 9.0	-0.675 ± 0.109	0.092	0.058	0.041	0.027	0.022	0.022
10	9.0 – 13.0	0.089 ± 0.193	0.161	0.107	0.067	0.063	0.038	0.039
11	13.0 – 20.0	0.243 ± 0.435	0.240	0.363	0.145	0.226	0.080	0.231

D^0 trajectory to a vertex, constrained to lie in the e^+e^- interaction region (smeared in the $r - \phi$ plane to account for the B flight length); we require $\chi^2/n_{dof} < 75$.

The remaining tracks are used to determine the second B decay vertex and its flavour, using the method of Ref. [16]. Events are classified into six subsets according to the purity of the tag. In this analysis we use only leptonic tags from the highest purity subset.

In total, 8565 events are selected (6718 OF, 1847 SF). A GEANT-based Monte Carlo (MC) sample assuming QM correlation, with five times the number of events, was analysed with identical criteria; its Δz and D^* mass distributions were tuned to those of the data. This sample was used for consistency checks, background estimates and subtraction, and to build deconvolution matrices.

To compensate for the rapid fall in event rate with Δt , the time-dependent distributions are histogrammed in 11 variable-size bins (Table I). Background subtraction is then performed bin-by-bin; systematic errors are likewise determined by estimating variations in the OF and SF distributions, and calculating the effect on the asymmetry. Terms due to event selection are estimated by comparing data and MC distributions for each quantity, and converting discrepancies into yield variations: effects due to each selection are added in quadrature. Estimation of the remaining terms is described below.

Four types of background event have been considered: $e^+e^- \rightarrow q\bar{q}$ continuum, fake D^* , wrong D^* -lepton combinations, and $B^+ \rightarrow \overline{D}^{**0}\ell\nu$ events. Off-resonance data (8.3 fb^{-1}) were used to estimate the continuum background, which was found to be negligible.

Fake D^0 reconstruction and misassigned slow pions produce a fake D^* background. We subtract 126 ± 6 (54 ± 4) such OF (SF) events based on scaled yields from the sideband $M_{\text{diff}} \in [156.0, 164.0] \text{ MeV}/c^2$. The corresponding systematic uncertainty is estimated by considering statistical fluctuations, and moving cuts by $\pm 0.02 \text{ MeV}/c^2$ (the estimated mis-calibration in M_{diff}). Alternate sidebands $[152.0, 156.0]$ and $[164.0, 168.0] \text{ MeV}/c^2$ are also used: the difference from default results (consistent with statistical fluctuations) is conservatively included in the systematic error.

The wrong D^* -lepton combination background is mainly due to the combination of a D^* from one B with a true lepton from the other B , with a smaller fraction due to fake leptons, and from charm decay. To estimate this background, for each selected $D^*\ell$ we reverse the lepton momentum vector in the CMS, labelling the modified lepton ℓ' , and require $|\cos(\theta_{B,D^*\ell'})| < 1.1$.

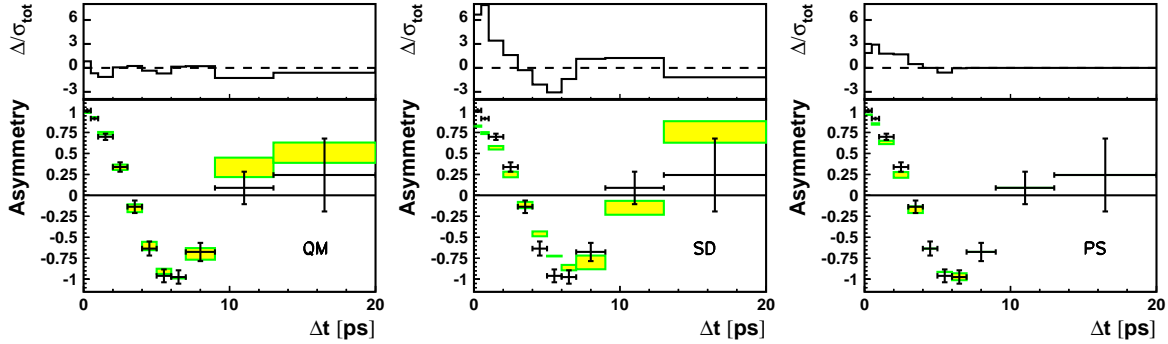


FIG. 2: Bottom: time-dependent flavour asymmetry (crosses) and the results of weighted least-squares fits to the (left to right) QM, SD, and PS models (rectangles, showing $\pm 1\sigma$ errors on Δm_d). Top: differences $\Delta \equiv A_{\text{data}} - A_{\text{model}}$ in each bin, divided by the total experimental error σ_{tot} . Bins where $A_{\text{PS}}^{\text{min}} < A_{\text{data}} < A_{\text{PS}}^{\text{max}}$ have been assigned a null deviation: see the text.

This procedure, intended to reject correlated $D^*\ell$ pairs while selecting events with no angular correlation, has been validated on MC events where true $B^0 \rightarrow D^{*-}\ell^+\nu$ combinations have been excluded. (The correlated background from charm decays is negligible.) We obtain 78 ± 9 OF and 237 ± 15 SF events, which are then subtracted. Contributions to the systematic error are obtained by considering the statistical fluctuations and by moving cuts by ± 0.1 to account for possible data-MC discrepancies.

After these subtractions, three main types of events remain: $B^0 \rightarrow D^{*-}\ell^+\nu$, the signal; $B^0 \rightarrow D^{**-}\ell^+\nu$, which we retain because it undergoes mixing; and $B^+ \rightarrow \overline{D}^{**0}\ell^+\nu$ background. MC shapes for the signal and the sum of the D^{**} channels are used in a two-parameter fit to the $\cos(\theta_{B,D^*})$ distribution to find the total D^{**} contribution ($\chi^2/n_{\text{dof}} = 56/46$), and its B^+ component is then estimated using MC fractions. We find 255.5 ± 16.0 events (254.0 OF and 1.5 SF), which we subtract from the data. The systematic uncertainty is estimated by adding in quadrature the fit error (6%) and variations obtained by moving the fit region (3%) and changing to a single parameter fit with forced normalisation (2%). We also assign a 20% uncertainty on the ratio of branching fractions of $B^0 \rightarrow D^{**-}\ell^+\nu$ to $B^+ \rightarrow \overline{D}^{**0}\ell^+\nu$.

We correct for wrong flavour assignments using OF and SF distributions from wrongly-tagged MC events. The mistag fraction 0.015 ± 0.001 (stat) is consistent with that in data [15]; we assign a systematic error of ± 0.005 .

Remaining reconstruction effects (e.g. resolution in Δt , selection efficiency) are corrected by deconvolution, treating the SF and OF distributions separately. The method is based on Deconvolution with Singular Value Decomposition (DSVD) [17]; 11×11 response matrices are built separately for SF and OF events, using MC $D^*\ell\nu$ events indexed by generated and reconstructed Δt values. The procedure has been optimised by a Toy Monte Carlo (TMC) technique where sets of several hundred simulated experiments are generated with data and MC samples identical in size to those of the real experiment, but assuming different true asymmetries A_{QM} , A_{SD} , and $A_{\text{PS}}^{\text{max}}$. In particular the following points have been studied:

- (1) The effective matrix rank was reduced from 11 to 5 (6) for the OF (SF) sample, to minimize the total error. (The statistical precision of some singular values is poor.)
- (2) The MC events used to fill the response matrix, and provide an *a priori* to the regularization algorithm, introduce a potential bias: *e.g.* the first Δt bin contains few SF events for QM, but is well-populated for SD. We therefore replace SF and OF samples with mixtures SF + $o \times$ OF and OF + $s \times$ SF, choosing $s = o = 0.2$ to minimize systematic effects; the exact values are not critical.
- (3) After DSVD, measured differences from input values are averaged (over QM, SD, and PS)

and subtracted bin-by-bin from the asymmetry, to reduce the potential bias against any one model. The maximal absolute deviation of the corrected distribution from the three models is assigned as the systematic error in each Δt bin.

(4) A $46\,\mu\text{m}$ Gaussian smearing term, inferred from the difference between MC and data vertex-fit errors, is used to tune the MC Δz distribution to the data. (The average Δz resolution is $\approx 100\,\mu\text{m}$). This term was varied by its $\pm 35\,\mu\text{m}$ uncertainty, and the resulting bin-by-bin difference in the asymmetry taken as the systematic error.

Terms from (3) and (4) are added in quadrature to give the total systematic error due to deconvolution. We test the consistency of the method by fitting the B^0 decay time distribution (summing OF and SF samples), leaving the B^0 lifetime as a free parameter. We obtain $1.532 \pm 0.017(\text{stat})\,\text{ps}$, consistent with the world average [11]. We also repeat the deconvolution procedure using events with better vertex fit quality, and hence more precise Δt values: consistent results are obtained.

The final results, which may be directly compared with theoretical models, are shown in Table I; addition in quadrature is used to combine the various error terms.

We perform weighted least-squares fits to $A(\Delta t)$, including a term taking the world-average Δm_d into account. To avoid bias we discard BaBar and Belle measurements, which assume QM correlations: this yields $\langle \Delta m_d \rangle = (0.496 \pm 0.014)\,\text{ps}^{-1}$ [19].

In fits to the QM, SD, and PS predictions, we obtain $\Delta m_d = 0.501 \pm 0.009$, 0.419 ± 0.008 , and $0.447 \pm 0.010\,\text{ps}^{-1}$ with χ^2 of 5.2, 174, and 31.3 respectively, for eleven degrees of freedom: see Fig. 2. The data favour QM over the SD model at 13σ , and QM over the PS model at 5.1σ [18]. As noted above, CP violation in mixing can be neglected. Introducing a lifetime difference $\frac{\Delta\Gamma_d}{\Gamma_d} = 0.009 \pm 0.037$ [19] has a negligible effect on the fit. As a consistency check, the time-dependent asymmetry before deconvolution is compared to MC predictions for QM and (*via* reweighting) the SD and PS models: QM is strongly favoured.

A further study of decoherence was performed by assuming that only a fraction of the neutral B pairs from $\Upsilon(4S)$ decays disentangle immediately into a B^0 and a \overline{B}^0 . To estimate this fraction we have fitted our asymmetry with a mixture $(1 - \lambda)A_{\text{QM}} + \lambda A_{\text{SD}}$. The fit finds $\lambda = 0.029 \pm 0.057$, consistent with no decoherence.

In summary, we have analysed neutral B pairs produced by $\Upsilon(4S)$ decay, determined the time-dependent asymmetry due to flavour oscillations, and corrected for experimental effects by deconvolution: the results can be directly compared to theoretical models. The local realistic model of Pompili and Selleri is strongly disfavoured compared to the entanglement predicted by quantum mechanics. Immediate disentanglement, in which definite-flavour B^0 and \overline{B}^0 evolve independently, is ruled out; if a fraction of B -pairs is assumed to decay incoherently, we find a decoherent fraction consistent with zero.

We thank P. Eberhard, G. Garbarino, B. Hiesmayr, A. Pompili, and F. Selleri for insightful discussions, the KEKB group for excellent operation of the accelerator, the KEK cryogenics group for efficient solenoid operations, and the KEK computer group and the NII for valuable computing and Super-SINET network support. We acknowledge support from MEXT and JSPS (Japan); ARC and DEST (Australia); NSFC and KIP of CAS (China); DST (India); MOEHRD, KOSEF and KRF (Korea); KBN (Poland); MIST (Russia); ARRS (Slovenia); SNSF (Switzerland); NSC and MOE (Taiwan); and DOE (USA).

[1] A. Einstein, B. Podolski and N. Rosen, Phys. Rev. **47**, 777 (1935).
[2] J. S. Bell, Physics **1**, 195 (1964).

- [3] R. A. Bertlmann and A. Zeilinger (eds.), *Quantum (Un)speakables: from Bell to Quantum Information*, Springer, Berlin, (2002), and references within.
- [4] A. Apostolakis *et al.* (CPLEAR Collaboration), Phys. Lett. B **422**, 339 (1998); R.A. Bertlmann, W. Grimus and B. C. Hiesmayr, Phys. Rev. D **60**, 114032 (1999); F. Ambrosino *et al.* (KLOE Collaboration), Phys. Lett. B **642**, 315 (2006).
- [5] R. A. Bertlmann, A. Bramon, G. Garbarino and B. C. Hiesmayr, Phys. Lett. A **332**, 355 (2004).
- [6] A. Datta and D. Home, Phys. Lett. A **119**, 3 (1986).
- [7] N. Gisin and A. Go, Am. J. Phys. **69** (3), 264 (2001).
- [8] The model is inspired by Furry's solution of the EPR paradox, in W. H. Furry, Phys. Rev. **49**, 393 (1936).
- [9] R. Omnès, Rev. Mod. Phys **64**, 339 (1992).
- [10] A. Pompili and F. Selleri, Eur. Phys. J. C **14**, 469 (2000); Frascati Physics Series Vol.XXVI 329 (2001).
- [11] Particle Data Group, W. -M. Yao *et al.*, J. Phys. G **33**, 1 (2006).
- [12] S. Kurokawa and E. Kikutani, Nucl. Instr. Meth. A **499** 1 (2003), and other papers in this volume.
- [13] A. Abashian *et al.* (Belle Collaboration), Nucl. Instr. Meth. A **479**, 117 (2002).
- [14] K. Hara *et al.* (Belle Collaboration), Phys. Rev. Lett. **89**, 251803 (2002).
- [15] K. Abe *et al.* (Belle Collaboration), Phys. Rev. D **71**, 072003 (2005).
- [16] K. Abe *et al.* (Belle Collaboration), Phys. Rev. Lett. **87**, 091802 (2002); Phys. Rev. D **66**, 32007 (2002); H. Kakuno *et al.*, Nucl. Instr. Meth. A **533**, 516 (2004).
- [17] A. Höcker and V. Kartvelishvili, Nucl. Instr. Meth. A **372**, 469 (1996).
- [18] For the PS fit, we assign a null deviation when the data falls within the PS range, otherwise the deviation is computed with respect to the closest boundary: A_{PS}^{\max} [Eq. (3)] or A_{PS}^{\min} [Eq. (4)].
- [19] E. Barberio *et al.* (Heavy Flavour Averaging Group), hep-ex/0603003 (2006).